

# Performance Analysis of Decouple-and-Forward MIMO Relay Systems in Rayleigh Fading

Jovan Stosic\*, Zoran Hadzi-Velkov†

## Abstract

In this paper we analyze the ergodic capacity and outage probability for a decouple-and-forward (DCF) MIMO relaying system with three nodes and direct link between the source and destination over a Rayleigh fading. The nodes employ multiple antennas and orthogonal space-time block coding (OSTBC). In the DCF relay, the incoming signal is decoupled, amplified and forwarded to the destination. Under assumption that source and destination have full CSI (Channel State Information) for source-relay, relay-destination and source-destination links we derive simple expressions for approximation of the ergodic capacity and outage probability. By means of these approximations it is shown that the system with direct link has better capacity and outage performance. For all considered scenarios the increase of the number of antennas per node results in increase of the ergodic capacity, decrease of the outage probability and increase of the diversity gain.

## 1 Introduction

Multiple-input multiple-output (MIMO) technology offers significant performance improvements in terms of capacity and reliability of wireless communications systems, achieved through exploiting the multipath propagation nature of the wireless transmission. The MIMO technology is currently deployed in wireless LANs (IEEE 802.11n and 802.11ac) and in LTE. Motivated in part by the MIMO concept, cooperative communications have emerged as breakthrough concept in wireless communications by offering additional capacity and reliability improvements at the cost of small additional signal processing [1]-[2]. Combined MIMO and cooperative relaying techniques offer high diversity and multiplexing gains at reduced transmit powers and decreased interference levels among the neighboring nodes.

There are two main relaying techniques, amplify-and-forward (AF) and decode-and-forward (DF). In the case of AF, the relay amplifies and forwards the received signal from the source, and in the case of DF the relay fully decodes the received signal and forwards it to the next hop. In this paper we utilize an AF technique for the MIMO relaying system, termed as the

---

\*Makedonski Telekom AD, Skopje, Macedonia; jstosic@t.mk

†Faculty of Electrical Engineering and Information Technology, Ss. Cyril and Methodius University, Skopje, Macedonia; zoranhv@feit.ukim.edu.mk,

Decouple-and-forward (DCF) relaying [3]. The DCF relaying system employs orthogonal space time block (OSTB) coding and decoding at the nodes, such that the relay first decodes (decouples) the incoming OSTB signal from the source, amplifies the de-coupled streams, and then OSTB re-encodes and forwards the amplified signal to the destination.

Numerous papers have been published in the topic of DCF relaying (e.g. [3]-[27]). An approximate and asymptotic bit error probability (BEP) analysis for distributed space time cooperative systems with a single-antenna source, two single-antenna relays, and a single-antenna destination is provided in [4]. A BEP analysis for a dual-hop MIMO systems using OSTBC with a multiple-antenna source, a single/multiple-antenna destination and a single-antenna relay is provided in [3] and [5]. The analysis in [6] extends the analysis in [3] for a DCF MIMO relay system where the source, the relay, and the destination have two antennas each. The paper [7] extends [3] and [6] by establishing an upper BEP bound for a multiple-antenna source, relay and destination. The authors in [8] found the exact and asymptotic expressions of the outage and error performance for a system with a single-antenna DCF relay, a multiple-antenna source and a multiple-antenna destination by employing OSTB codes in Nakagami-m fading. The error performance for the DCF MIMO relay system with multiple antennas in each node is presented in [9], which also provides a comparison with a MIMO relay system with and without relay selection. Accurate expressions and bounds of outage probability of a DCF MIMO relay system with two antennas per node over a Nakagami-m fading environment is provided in [10]. In the paper [11] lower bound error performance has been analyzed in a distributed space-time block code system with a direct link between the dual-antenna source and destination and an indirect link through a multiple-antenna relay. The paper [12] presents performance analysis of dual-hop DCF MIMO relay systems where each node has multiple antennas. The papers [13] and [14] provide tight approximations for the error and outage probability of dual-hop DCF MIMO relay systems in Rayleigh fading. The paper [15] provides exact ergodic capacity for DF relay system with single antenna at each node and no direct link in Rician Fading. The authors of [16] derive a closed-form expression of MGF (Moment Generating Function) of the instantaneous SNR for hop-by-hop beamforming and combining in a dual-hop AF MIMO relay network with two antennas in each node over Nakagami-m fading. They extend the analysis in [17] by providing the approximate average error rate expressions. The paper [18] provides tight approximations for the MGF of the instantaneous SNR in two-way AF MIMO relay system with estimated CSI in Rayleigh fading. The authors of [19] present error rate analysis of DF MIMO relay network with beamforming and transmission path selection in Rayleigh Fading. The paper [20] provides expressions of the average error probability for piece-wise linear decoder for MIMO cooperative system with single and multiple MIMO relays. The authors of [21] derive the approximate expression for the symbol error rate of AF MIMO relay network in Rayleigh fading for M-ary phase shift keying. The authors of [22] analyze three different decoders and for one of them they derive MGF of the instantaneous SNR for AF MIMO relay network. The paper [23] proposes a joint decoder for two-way AF based MIMO cooperative system and derive the closed-form expression for MGF of the instantaneous SNR in Rayleigh

fading. The authors of [24] provide error rate performance analysis of the AF MIMO relay network with imperfect CSI.

Most of the aforementioned papers which focus on MIMO relay systems provide only error or outage probability performance analysis. Similarly to the referenced works, we focus on the AF MIMO relay system, which utilizes the "Decouple-and-Forward" relaying. For such system, we present approximate expressions for the ergodic capacity, which is novel analysis in the literature. Additionally, we also present outage probability analysis for this system, along with simple approximations for the outage probability.

The remainder of this paper is organized as follows. Next section presents the system model and the signal processing at the nodes. In Section 3 we derive the simple approximations for the ergodic capacity, whereas respective approximations for the outage probability are presented in Section 4 and Section 5 concludes the article.

## 2 System model

In this paper it is assumed that the source, the half-duplex DCF relay and the destination are equipped with multiple antennas and operate in Rayleigh fading environment. As depicted in Fig. 1, we consider a system that consists of a source with  $N$  antennas (denoted as the node 1), a half-duplex DCF relay with either a single or  $N$  antennas (denoted as the node 2), and a destination with  $N$  antennas (denoted as the node 3). Each of the three nodes utilizes OSTB coding.

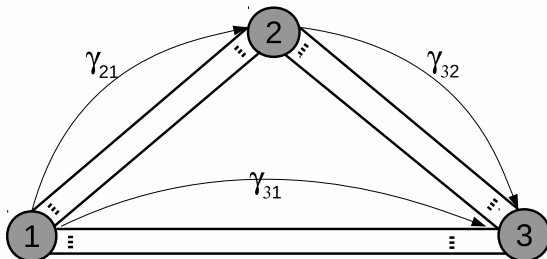


Figure 1: Dual-hop DCF MIMO relay system with direct link to the destination

We consider 3 system configurations: (1)  $N \times 1 \times N$  configuration without a direct link, where the source and destination are equipped with  $N$  antennas whereas the relay has a single antenna; (2)  $N \times N \times N$  configuration without a direct link, where the three nodes are equipped with  $N$  antennas; and (3)  $N \times N \times N$  configuration with a direct link.

The source-relay, relay-destination and source-destination links are exposed to random fading. In particular, the channels are modeled as independent MIMO Rayleigh block fading channels with channel matrices  $\mathbf{H} = [h_{ij}]$ ,  $\mathbf{G} = [g_{ij}]$  and  $\mathbf{W} = [w_{ij}]$ , respectively. The channel coefficient between the  $i$ -th antenna of the source and the  $j$ -th antenna of the relay is denoted by  $h_{ij}$ , the channel coefficient between the  $i$ -th antenna of the relay and the  $j$ -th antenna of the destination is denoted by  $g_{ij}$ , and the channel coefficient between the  $i$ -th antenna of the source and the  $j$ -th antenna of the destination is denoted by  $w_{ij}$ . The channel coefficients  $h_{ij}$ ,  $g_{ij}$  and  $w_{ij}$  are

circularly symmetric complex Gaussian random variables with zero mean and unit variance, i.e.,  $h_{ij} \sim \mathcal{CN}(0, 1)$ ,  $g_{ij} \sim \mathcal{CN}(0, 1)$  and  $w_{ij} \sim \mathcal{CN}(0, 1)$  [28]. Since the channels are assumed to be block fading,  $h_{ij}$ ,  $g_{ij}$  and  $w_{ij}$  are constant in one block, but change from one block to the next. In each fading block, the relay is assumed to know channel matrix  $\mathbf{H}$ , whereas the destination is assumed to know channel matrices  $\mathbf{G}$  and  $\mathbf{W}$  [29]. In the system configuration (1),  $\mathbf{H}$ ,  $\mathbf{G}$  and  $\mathbf{W}$  are  $N \times 1$  vectors. In the system configurations (2) and (3),  $\mathbf{H}$ ,  $\mathbf{G}$  and  $\mathbf{W}$  are  $N \times N$  matrices.

We assume the operation of the DCF MIMO relaying system is divided into transmission epochs of equal duration. One transmission epoch coincides with one fading block. Each epoch is divided into 2 phases of equal duration: in phase 1, the source transmits towards the destination and/or the relay, and in phase 2, the relay forwards the processed signal received in the previous phase towards destination.

## 2.1 Signal Processing

In phase 1, the source transmits a sequence of multiple OSTB codewords. Each OSTB codeword combines  $K$  information symbols, transmitted over  $N$  transmit antennas during  $L$  time sub-slots. Depending on the application's delay tolerance, the OSTB sequence in phase 1 may consist of a single codeword (i.e., the non-ergodic scenario considered in Section 4), or be a part of a single long codeword that spans many fading blocks (i.e., the ergodic scenario considered in Section 3). Combining of the  $K$  information symbols  $\mathbf{X} = [x_1, x_2, \dots, x_K]^T$  is according to a particular OSTB coding scheme (as per Section 2.2) [30]. The OSTB coding schemes are designated by using a three-digit number "NKL". In the phase 2, the relay decouples separately each OSTB codeword from the packet received in phase 1.

On the symbol basis, given system configurations (2) and (3), the relay decouples the received signal  $Y$ , amplifies each of the decoupled symbols, encodes and forwards them as a new OSTB codeword. The new OSTB codeword is obtained from a group of  $K$  decoupled information symbols  $\tilde{\mathbf{X}} = [\tilde{x}_1, \tilde{x}_2, \dots, \tilde{x}_K]^T$  sent over  $N$  transmit antennas in  $L$  successive time slots. In case of the system configuration (1), the relay forwards the decoupled information symbols  $\tilde{\mathbf{X}}$  without employment of OSTB codes, in which case the destination combines the signals from its multiple antennas by using maximum ratio combining (MRC).

At the end of phase 1, the received signal at single relay antenna is given by

$$\mathbf{Y} = \sqrt{E_s} \mathbf{C} \mathbf{H} + \mathbf{N}, \quad \mathbf{Y} = [y_1, y_2, \dots, y_L]^T, \quad (1)$$

where  $\mathbf{C}$  is  $L \times N$  codeword matrix of the OSTB code given by (14) for the 3 considered codes, and  $\mathbf{N}$  is  $L \times 1$  vector and denotes the additive white Gaussian noise (AWGN) at the relay, whose elements are circularly symmetric complex Gaussian random variables with zero mean and variance  $N_0$ . In (1)  $E_s$  is the average transmitted power per symbol. For the OSTB

codewords given by (14), the average power per symbol is calculated as

$$E_s = \frac{L}{K N} P, \quad (2)$$

where  $P$  is the total transmit power of the source.

The relay decouples the received signal from the source, such that each decoupled symbol is represented as the sum of the faded symbol transmitted from the source and the additive white Gaussian noise. De-coupling at the relay for the 3 OSTB codes is given by (15) of the following subsection. In [31, sec.(4)] it is shown that the particular decoupled symbol at the relay is given by

$$\tilde{x}_k = \sqrt{E_s} \|\mathbf{H}\|_F^2 x_k + \xi_k, \quad k = 1, 2, \dots, K, \quad (3)$$

$$\text{where, } \|\mathbf{H}\|_F^2 = \begin{cases} \sum_{i=1}^N |h_i|^2 & \text{for system configuration (1)} \\ \sum_{i=1}^N \sum_{j=1}^N |h_{ij}|^2 & \text{for system configurations (2) and (3)} \end{cases}, \quad (4)$$

is the squared Frobenius norm [32, eq.(2.3.1)] of the channel matrix  $\mathbf{H}$ ,  $\xi$  is complex-valued AWGN with zero mean and variance  $\|\mathbf{H}\|_F^2 N_0$ . The relay amplification factor is adjusted so as to maintain the constant value of the relay's output power

$$A = \sqrt{\frac{E_2}{(E_1 \|\mathbf{H}\|_F^4 + \|\mathbf{H}\|_F^2 N_0)}}, \quad (5)$$

where transmitted symbol energies from the source and the relay are assumed to be equal i.e.  $E_1 = E_2 = E_s$ . For fair comparison, the relay's total output power should be the same for all system configurations, and therefore the relay's output power for system configuration (1) must be normalized by the power normalization factor  $b$  ( $0 < b \leq 1$ ). Furthermore, we can approximate (5) by neglecting its AWGN term, which yields

$$A \approx \frac{1}{\sqrt{b} \|\mathbf{H}\|_F^2}, \quad (6)$$

$$\text{where, } b = \begin{cases} L/(K N) & \text{for system configuration (1)} \\ 1 & \text{for system configurations (2) and (3)} \end{cases}. \quad (7)$$

Similarly as in (3), the decoupled symbols at the destination are given by

$$\hat{x}_k = A \|\mathbf{G}\|_F^2 \tilde{x}_k + \mu_k, \quad k = 1, 2, \dots, K, \quad (8)$$

$$\text{where, } \|\mathbf{G}\|_F^2 = \begin{cases} \sum_{i=1}^N |g_i|^2 & \text{for system configuration (1)} \\ \sum_{i=1}^N \sum_{j=1}^N |g_{ij}|^2 & \text{for system configurations (2) and (3)} \end{cases}, \quad (9)$$

is the squared Frobenius norms of the channel matrix  $\mathbf{G}$ , and  $\mu$  is complex-valued AWGN with

zero mean and variance  $\|\mathbf{G}\|_F^2 N_0$ . By introducing (3) into (8), we obtain

$$\hat{x}_k = \sqrt{E_s} A \|\mathbf{H}\|_F^2 \|\mathbf{G}\|_F^2 x_k + A \|\mathbf{G}\|_F^2 \xi_k + \mu_k. \quad (10)$$

Therefore, in a given fading state, when  $\mathbf{H}$  and  $\mathbf{G}$  are constant, the instantaneous powers of the desired signal and the AWGN at the destination is given by

$$\begin{aligned} P_S &= E_s A^2 \|\mathbf{H}\|_F^4 \|\mathbf{G}\|_F^4, \\ P_N &= A^2 \|\mathbf{G}\|_F^4 \|\mathbf{H}\|_F^2 N_0 + \|\mathbf{G}\|_F^2 N_0. \end{aligned} \quad (11)$$

In the remainder of this paper, we designate the total average SNR by  $\rho$  and the average signal-to-noise ratio (SNR) per symbol by  $\bar{\gamma} = E_s/N_0 = b\rho$ . Then the instantaneous SNR of the direct link is given by  $\gamma_{31} = \bar{\gamma} \|\mathbf{W}\|_F^2$ , the instantaneous SNR of the source-relay link is given by  $\gamma_{21} = \bar{\gamma} \|\mathbf{H}\|_F^2$ , and the instantaneous SNR of the relay-destination link is given by  $\gamma_{32} = \bar{\gamma} \|\mathbf{G}\|_F^2$ . By introducing (5) into (11), the instantaneous SNR per symbol for configurations (1) and (2) is given by

$$\gamma = \frac{P_S}{P_N} = \frac{E_s}{N_0} \frac{A^2 \|\mathbf{G}\|_F^2 \|\mathbf{H}\|_F^4}{A^2 \|\mathbf{G}\|_F^2 \|\mathbf{H}\|_F^2 + 1} = \frac{\gamma_{21} \gamma_{32}}{\gamma_{21} + \gamma_{32} + 1}. \quad (12)$$

By applying (6) into (11) instantaneous SNR for configurations (1) and (2) is

$$\gamma = \frac{\gamma_{21} \gamma_{32}}{\gamma_{21} + \gamma_{32}}. \quad (13)$$

## 2.2 OSTB coding scheme examples

We focus on three practical OSTBC schemes, "222", "334" and "434", applied in the considered system. OSTB coding matrices for schemes "222", "334" and "434" are respectively given by [30] [33]

$$\begin{aligned} \mathbf{C}_{222} &= \begin{bmatrix} x_1 & x_2 \\ -x_2^* & x_1^* \end{bmatrix}, \quad \mathbf{C}_{334} = \begin{bmatrix} x_1 & x_2 & x_3 \\ -x_2^* & x_1^* & 0 \\ x_3^* & 0 & -x_1^* \\ 0 & x_3^* & -x_2^* \end{bmatrix}, \\ \mathbf{C}_{434} &= \begin{bmatrix} x_1 & x_2 & x_3/\sqrt{2} & x_3/\sqrt{2} \\ -x_2^* & x_1^* & x_3/\sqrt{2} & -x_3/\sqrt{2} \\ x_3/\sqrt{2} & x_3/\sqrt{2} & \frac{(-x_1-x_1^*+x_2-x_2^*)}{2} & \frac{(-x_2-x_2^*+x_1-x_1^*)}{2} \\ x_3^*/\sqrt{2} & -x_3^*/\sqrt{2} & \frac{(x_2+x_2^*+x_1-x_1^*)}{2} & -\frac{(x_1+x_1^*+x_2-x_2^*)}{2} \end{bmatrix} \end{aligned} \quad (14)$$

The signal processing (i.e., symbol decoupling) at a single relay antenna for OSTB codes in (14) is given by the following vectors [30] [31]

$$\begin{aligned}
\tilde{\mathbf{X}}_{222}^T &= [y_1 h_1^* + y_2^* h_2, y_1 h_2^* - y_2^* h_1], \\
\tilde{\mathbf{X}}_{334}^T &= [y_1 h_1^* + y_2^* h_2 - y_3^* h_3, y_1 h_2^* - y_2^* h_1 - y_4^* h_3, y_1 h_3^* + y_3^* h_1 + y_4^* h_2], \\
\tilde{\mathbf{X}}_{434} &= \begin{bmatrix} y_1 h_1^* + y_2^* h_2 + \frac{(y_4 - y_3)(h_3^* - h_4^*)}{2} - \frac{(y_3^* + y_4^*)(h_3 + h_4)}{2} \\ y_1 h_2^* - y_2^* h_1 + \frac{(y_4 + y_3)(h_3^* - h_4^*)}{2} + \frac{(y_4^* - y_3^*)(h_3 + h_4)}{2} \\ \frac{(y_1 + y_2) h_3^*}{\sqrt{2}} + \frac{(y_1 - y_2) h_4^*}{\sqrt{2}} + \frac{(h_1 + h_2) y_3^*}{\sqrt{2}} + \frac{(h_1 - h_2) y_4^*}{\sqrt{2}} \end{bmatrix}. \quad (15)
\end{aligned}$$

For system configurations (2) and (3) the decoupled symbols per each additional relay antenna is obtained similarly as in (15). In that case the final expression of the decoupled symbol at the relay is obtained by summing the decoupled symbols in each of the  $N$  relay antennas.

### 3 Capacity in ergodic scenario

The ergodic capacity is the maximal achievable rate of a communication system in an ergodic channel [42, eq.(5.89)][43, eq.(4.4)]

$$C = E [\log_2(1 + \gamma)] = \int_0^\infty \log(1 + \gamma) f(\gamma) d\gamma \quad \text{bits/sec/Hz}, \quad (16)$$

where  $\gamma$  is instantaneous SNR before the receiver and  $E[\cdot]$  denotes the expectation. From a practical aspect the ergodic capacity can be achieved by using very long codewords that span many fading states, which is appropriate for delay-tolerant applications. In this case, both the transmitter and the receiver have the same codebook available, which consist of  $2^{n^C}$  codewords. By combining (16) and [44, eq.(4)], the ergodic capacity of the point-to-point MIMO system with OSTBC is

$$C = E \left[ \frac{K}{L} \log_2(1 + \gamma) \right]. \quad (17)$$

Since the symbol transmission takes two phases the ergodic capacity of configurations (1), (2) and (3) is obtained by dividing (17) by factor of 2 i.e.

$$C = \frac{1}{2} E \left[ \frac{K}{L} \log_2(1 + \gamma) \right] \quad (18)$$

For general system which includes all three configurations the instantaneous SNR  $\gamma$  is a sum of the instantaneous SNR of the direct link  $\gamma_{31}$  and the instantaneous SNR of the indirect link  $\gamma_R$  (given with (13)) [34, eq.(16.18)], [39, eq.(12)]

$$C = \frac{1}{2} E \left[ \frac{K}{L} \log_2(1 + \gamma_{31} + \gamma_R) \right]. \quad (19)$$

### 3.1 System configurations (1) and (2)

Since the direct link is not present, the ergodic capacity of system configurations (1) and (2) is obtained by taking  $\gamma_{31} = 0$  and  $\gamma_R = \gamma_{32} \gamma_{21} / (\gamma_{32} + \gamma_{21})$  in (19)

$$C^{(1,2)} = \frac{1}{2} E \left[ \frac{K}{L} \log_2 \left( 1 + \frac{\gamma_{32} \gamma_{21}}{\gamma_{32} + \gamma_{21}} \right) \right]. \quad (20)$$

As proven in the Appendix A the PDF of the instantaneous SNR at the destination  $\gamma_R$  for the system configurations (1) and (2) is given by the Gamma PDF [40, eq.(4-34)]

$$f(\gamma) = \frac{(b+1)^m}{\gamma^m \Gamma(m)} \gamma^{m-1} e^{-\frac{(b+1)\gamma}{\bar{\gamma}}} \quad \gamma \geq 0, \quad (21)$$

where  $b$  is given with (7) and

$$m = \begin{cases} N & \text{for system configuration (1)} \\ N^2 & \text{for system configuration (2)} \end{cases}. \quad (22)$$

Introducing (21) into (20), the ergodic capacity of system configurations (1) and (2) is

$$C^{(1,2)} = \frac{K}{2L\Gamma(m)\ln(2)} G_{3,2}^{1,3} \left( \frac{L\rho}{KN_T(b+1)} \Big|_{1,0}^{1-m,1,1} \right), \quad (23)$$

where  $\Gamma(\cdot)$  is the Gamma function, defined by [35, eq. (8.310.1)] and  $G_{3,2}^{1,3}(\cdot)$  is Meijer G function defined by [35, eq. (9.301)]. Note, according to (7) and (22),  $b = L/(KN)$  and  $m = N$  for system configuration (1), and  $b = 1$  and  $m = N^2$  for system configuration (2). To the best of author's knowledge, (23) is a novel result.

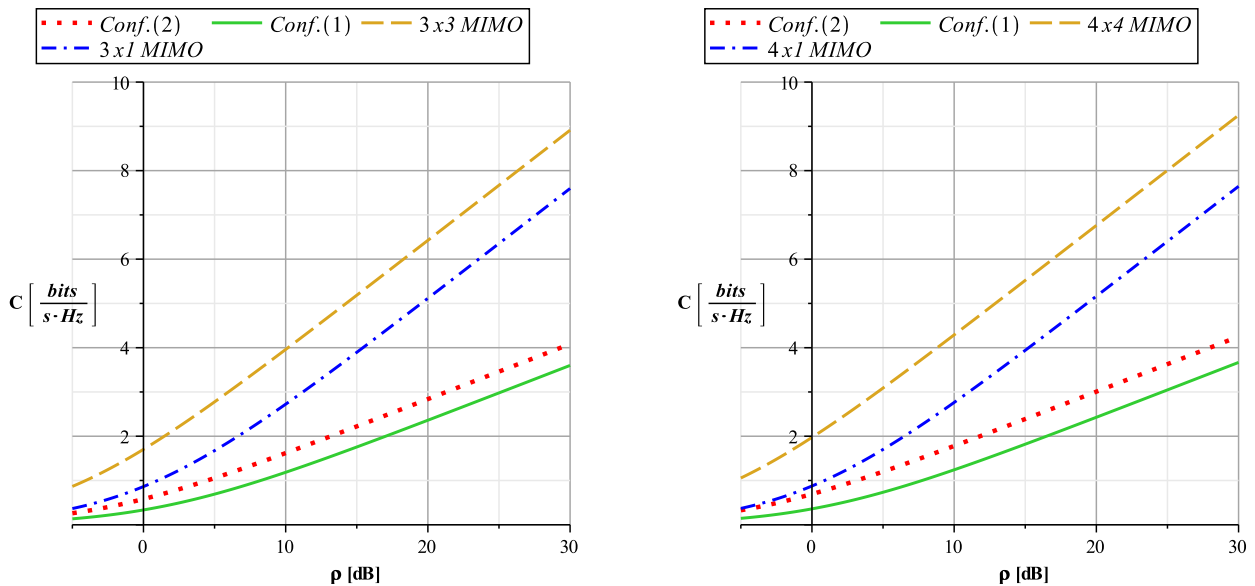


Figure 2: Ergodic capacity of configuration (1) and (2) for  $N = 3$  and  $N = 4$ .

In Fig.3.1 we compare the ergodic capacity of system configurations (1) and (2) given with (23) and ergodic capacity of point-to-point MIMO systems for  $N = 3$  and  $N = 4$ . The ergodic capacity of point-to-point MIMO system is obtained by taking  $b = 0$  in (23) and the curves in the figures for ergodic capacity of this system are designated by  $N_T \times N_R$  where  $N_T$  designates the number of antennas at the transmitter in the source and  $N_R$  designate the number of antennas at the receiver in the destination. The ergodic capacity of configurations (1) and (2) (obtained by (23)) doesn't surpass the ergodic capacity of the point-to-point MIMO system. The ergodic capacity of configurations (1) and (2) increase with increase of the number of antennas. For example, for configuration (2) the ergodic capacity for  $N = 4$  compared to the case where  $N = 3$  is higher for  $0.07 \text{ bits/s/Hz}$  on  $\rho = -5 \text{ dB}$  and  $0.17 \text{ bits/s/Hz}$  on  $\rho = 30 \text{ dB}$ . The ergodic capacity of the configuration (2) is higher then the ergodic capacity of the configuration (1). The performance gap is increased by increasing the average SNR and increasing the number of antennas. For example, the gap in the case of  $N = 3$  is  $0.16 \text{ bits/s/Hz}$  on  $\rho = -5 \text{ dB}$  and  $0.38 \text{ bits/s/Hz}$  on  $\rho = 30 \text{ dB}$ . In case of  $N = 4$  the gap is  $0.18 \text{ bits/s/Hz}$  on  $\rho = -5 \text{ dB}$  and  $0.58 \text{ bits/s/Hz}$  on  $\rho = 30 \text{ dB}$ .

### 3.2 System configuration (3)

Since the direct link is present i.e.  $\gamma_{31} \neq 0$ , the ergodic capacity of system configuration (3) is obtained by taking  $\gamma_R = \gamma_{32} \gamma_{21} / (\gamma_{32} + \gamma_{21})$  in (19)

$$C = \frac{1}{2} E \left[ \frac{K}{L} \log_2 \left( 1 + \gamma_{31} + \frac{\gamma_{21} \gamma_{32}}{\gamma_{21} + \gamma_{32}} \right) \right]. \quad (24)$$

As proven in the Appendix B, the instantaneous SNR of the received signal at the destination of the system configuration (3) is given by

$$f(\gamma) = \sum_{k=0}^{\infty} \frac{(m)_k}{k!} \frac{\gamma^{2m+k-1} 2^m}{\Gamma(2m+k) \bar{\gamma}^{2m+k}} e^{-\frac{2\gamma}{\bar{\gamma}}}. \quad (25)$$

where  $b = 1$ ,  $m = N^2$  and  $(m)_k$  is a Pochhammer symbol, defined by [41, eq.(2.12)].

By introducing (25) in (24) the ergodic capacity is obtained as

$$\begin{aligned} C^{(3)} &= \frac{1}{2} \sum_{k=0}^{\infty} \frac{(m)_k}{k!} \int_0^{\infty} \frac{\gamma^{2m+k-1} 2^m}{\Gamma(2m+k) \bar{\gamma}^{2m+k}} e^{-\frac{2\gamma}{\bar{\gamma}}} \frac{K}{L} \log_2(1 + \gamma) d\gamma \\ &= \frac{1}{2} \sum_{k=0}^{\infty} \frac{(m)_k}{k!} \int_0^{\infty} \frac{u^{2m+k-1} 2^m}{\Gamma(2m+k)} e^{-2u} \frac{K}{L} \log_2(1 + u \cdot \bar{\gamma}) du. \end{aligned} \quad (26)$$

Note, the second line of (26) is obtained by applying the substitution  $u = \gamma/\bar{\gamma}$ . For high average SNRs, i.e.  $\bar{\gamma} \rightarrow \infty$ , we can use approximation  $\log_2(1 + u\bar{\gamma}) \approx \log_2(u\bar{\gamma})$ , which yields

$$C^{(3)} \approx \frac{1}{2} \sum_{k=0}^{\infty} \frac{K (m)_k (\ln(\bar{\gamma}/2) + \Psi(2m+k))}{L k! \ln(2) 2^{m+k}}, \text{ as } \bar{\gamma} \rightarrow \infty, \quad (27)$$

where  $\Psi$  is a digamma function, defined by [36, eq.(6.3.1)]. For low average SNRs, i.e.  $\bar{\gamma} \rightarrow 0$  we use the approximation  $\log_2(1 + u\bar{\gamma}) \approx (u\bar{\gamma}) / \ln(2)$ , which yields

$$C^{(3)} \approx \frac{1}{2} \sum_{k=0}^{\infty} \frac{K(m)_k \bar{\gamma} (2m+k)}{\ln(2) L k! 2^{m+k+1}}, \text{ as } \bar{\gamma} \rightarrow 0. \quad (28)$$

To the best of author's knowledge, (26), (27) and (28) are novel results.

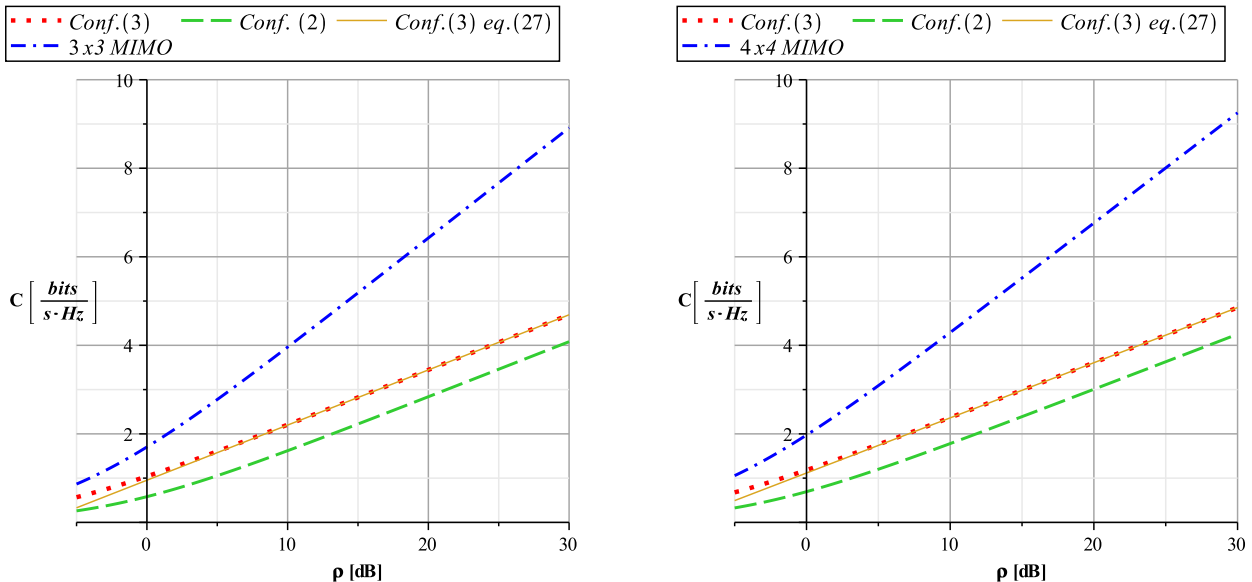


Figure 3: Ergodic capacity of configuration (2) and (3) for  $N = 3$  and  $N = 4$

Fig.3.2 depict ergodic capacity vs. average SNR  $\rho$ , where  $\rho = \frac{NK}{L} \bar{\gamma}$ . We observe that configuration (3) has higher ergodic capacity then the configuration (2) for all values of  $\rho$ . The performance gap between the two configurations for the case of  $N = 3$  is  $0.4 \text{ bits/s/Hz}$  on  $\rho = -5 \text{ dB}$  and  $0.6 \text{ bits/s/Hz}$  on  $\rho = 30 \text{ dB}$ . For the case of  $N = 4$  the gap is  $0.35 \text{ bits/s/Hz}$  on  $\rho = -5 \text{ dB}$  and  $0.57 \text{ bits/s/Hz}$  on  $\rho = 30 \text{ dB}$ . We observe minor decrease of the gap between the two configurations by increase of the number of antennas. Additionally we observe increase of capacity with increase of the number of antennas. For example, for the configuration (3) the increase of the capacity for  $N = 4$  in comparison to the  $N = 3$  is  $0.11 \text{ dB}$  on  $\rho = -5 \text{ dB}$  and  $0.13 \text{ dB}$  on  $\rho = 30 \text{ dB}$ . Moreover point-to-point MIMO system has slightly higher ergodic capacity in comparison to the configuration (3) for low values of the average SNR and significantly higher ergodic capacity for middle to high values of the average SNR. The performance gap between this two systems is slightly increased by increase of the number of antennas. In case of  $N = 3$  the gap is  $0.31 \text{ bits/s/Hz}$  on  $\rho = -5 \text{ dB}$  and  $4.213 \text{ bits/s/Hz}$  on  $\rho = 30 \text{ dB}$ . For the case of  $N = 4$  the gap is  $0.38 \text{ bits/s/Hz}$  on  $\rho = -5 \text{ dB}$  and  $4.394 \text{ bits/s/Hz}$  on  $\rho = 30 \text{ dB}$ . Note that the approximation (27) is tight for middle to high average SNR. Due to the complexity of (26) for obtaining the curves for configuration (3) in Fig.3.2 we used the first 50 most significant terms in the summation.

On the table 1 approximate value of ergodic capacity is obtained by (26) where first  $n$  terms of the summation are used, and accurate value of ergodic capacity is obtained by means of

numeric integration of (26) in computer algebra system. By increase of  $n$  we observe decrease of the relative error. Taking in the account that the mean absolute percentage error (MAPE) for  $N = 2$  is  $7.3077 \cdot 10^{-9}$  and for  $N = 3$  is  $1.9081 \cdot 10^{-4}$ , this additional approximation has negligible effect on the accuracy of the results.

$n = 10$	$n = 30$	$n = 50$
$3.3763 \cdot 10^{-1}$	$1.0634 \cdot 10^{-4}$	$6.3756 \cdot 10^{-5}$

Table 1: Relative error of (26) for different number of terms in the summation for  $N = 3$  and  $\rho = 10 \text{ dB}$

## 4 Outage probability in non-ergodic scenario

When the system does not tolerate significant delay, the transmitted codewords must have relatively short time duration, equal to the duration of one fading block (or, in this case, equal to the duration of one epoch). In this case, each codeword may be exposed to only a single fading state and its rate cannot guarantee a reliable transmission over that transmission epoch. In this case, capacity outages may occur, and the relevant performance metric is the so called *capacity outage probability*, simply denoted as the *outage probability* [42, eq.(5.54)]. Such channel cannot support a maximum error-free transmission rate (16). However, it can support any target rate  $R$  with possibility of occurrence of an outage event when the rate is greater than channel capacity ( $R > C$ ). The outage probability of such event is [42, eq.(5.54)]

$$P_{out} = Pr [C \leq R]. \quad (29)$$

### 4.1 System configuration (1) and (2)

For determining the outage probability, the considered relaying system is treated as a point-to-point system whose instantaneous SNR is given by (13). Since  $C = [K / (2L)] \log_2(1 + \gamma)$ , (29) is transformed as  $Pr \left[ \frac{K}{2L} \log_2(1 + \gamma) < R \right] = Pr [\gamma \leq \gamma_{th}]$ , where  $\gamma_{th} = 2^{\frac{2L}{K} R} - 1$ . The PDF of  $\gamma$  is given by (21), hence the outage probability is

$$\begin{aligned} P_{out}^{(1,2)} &= Pr [\gamma \leq \gamma_{th}] = 1 - \frac{(b+1)^m}{\bar{\gamma}^m \Gamma(m)} \int_{\gamma_{th}}^{\infty} \gamma^{m-1} e^{-\frac{(b+1)\gamma}{\bar{\gamma}}} d\gamma = \\ &= 1 - \frac{1}{\Gamma(m)} \Gamma \left[ m, \frac{(b+1) K N_T}{\rho L} \left( 2^{\frac{2L}{K} R} - 1 \right) \right] \end{aligned} \quad (30)$$

To the best of author's knowledge, (30) is a novel result.

The outage probability of system configuration (2) for  $N = 3$  and  $N = 4$  antennas in the source and destination for three different values of the rate  $R = 1, 2$ , and  $3 \text{ bits/s/Hz}$  is presented on the left and right of the Fig.4, correspondingly. The curves with solid and dash lines are related to the configuration (2) and the dotted curves are related to the Monte Carlo

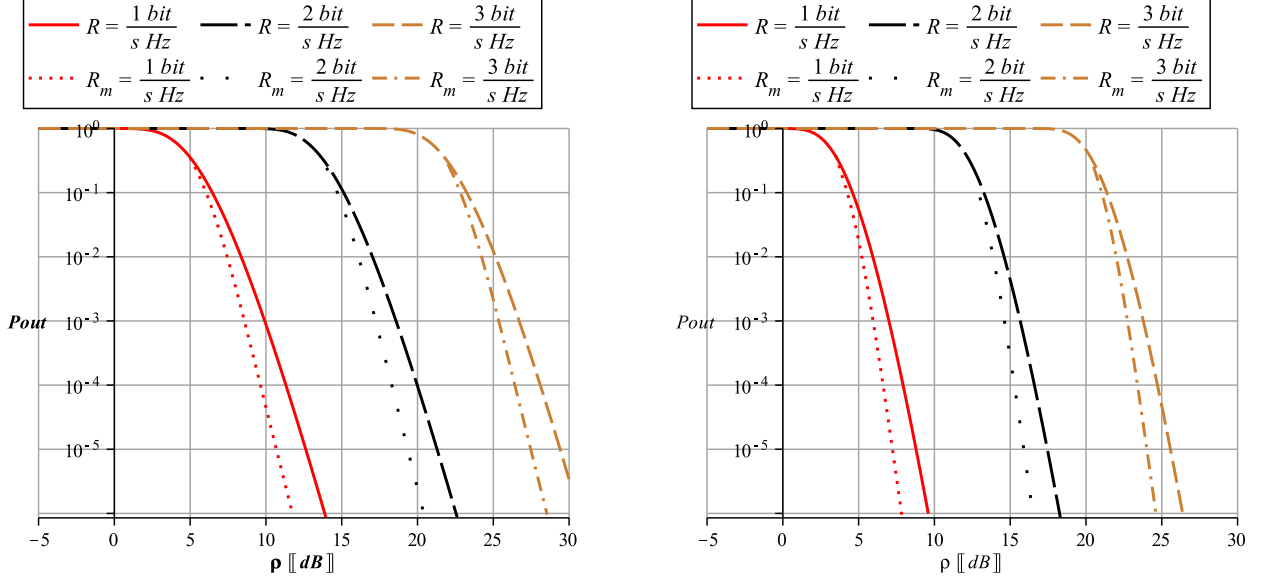


Figure 4: Outage probability of configuration (2) for  $N = 3$  and  $N = 4$  at different  $R$

simulations of the configuration (2)<sup>1</sup>. We observe good matching of the results obtained by approximation and the exact results obtained by a Monte Carlo simulation. If we compare the results for system configuration (2) for  $N = 3$  and  $N = 4$  antennas we conclude that the latter case has better performance. For example, in case of rate  $R = 2 \text{ bits/s/Hz}$  the outage probability of  $10^{-3}$  for the system with  $N = 3$  antenna is achieved at  $\rho = 18.5 \text{ dB}$  and for the system with  $N = 4$  antenna is achieved at  $\rho = 15.6 \text{ dB}$ . Additionally by usage of [38, eq.(5.2)] it can be found that diversity gain of the system with  $N = 4$  is  $d = 16$  which is almost twice as large as the diversity gain of the system with  $N = 3$  ( $d = 9$ ).

## 4.2 System configuration (3)

In this case, we introduce (25) in (29) to determine the outage probability

$$\begin{aligned}
 P_{out}^{(3)} = Pr[\gamma \leq \gamma_{th}] &= 1 - \sum_{k=0}^{\infty} \frac{\binom{m}{k}}{k!} \frac{1}{\Gamma(2m+k)} \int_{\gamma_{th}}^{\infty} \frac{\gamma^{2m+k-1} 2^m}{\bar{\gamma}^{2m+k}} e^{-\frac{2\gamma}{\bar{\gamma}}} d\gamma = \\
 &1 - \sum_{k=0}^{\infty} \frac{\binom{m}{k}}{k!} \frac{1}{2^{m+k}} \frac{1}{\Gamma(2m+k)} \Gamma\left(2m+k, 2 \frac{2^{\frac{LR}{K}} - 1}{\bar{\gamma}}\right)
 \end{aligned} \quad (31)$$

where  $\gamma_{th} = 2^{\frac{2L}{K}} R - 1$ . To the best of author's knowledge, this is a novel result.

On Fig.5 we compare the outage probability of configuration (3) given with (31), with outage probability of configuration (2) given with (30) for  $N = 3$  (left of Fig.5) and  $N = 4$  (right of Fig.5) for different rates ( $R = 1, 2, \text{ and } 3 \text{ bits/s/Hz}$ ). The curves with solid and dash lines are related to the configuration (3) and the dotted curves are related to the configuration (2)<sup>2</sup>. Configuration (3) has significantly lower outage probability than configuration (2). For  $N = 3$

<sup>1</sup>The designation of the rate have index "m", i.e.  $R_m$ .

<sup>2</sup>The designation of the rate have subscript related to the configuration e.g.  $R_{(2)}$  and  $R_{(3)}$ .

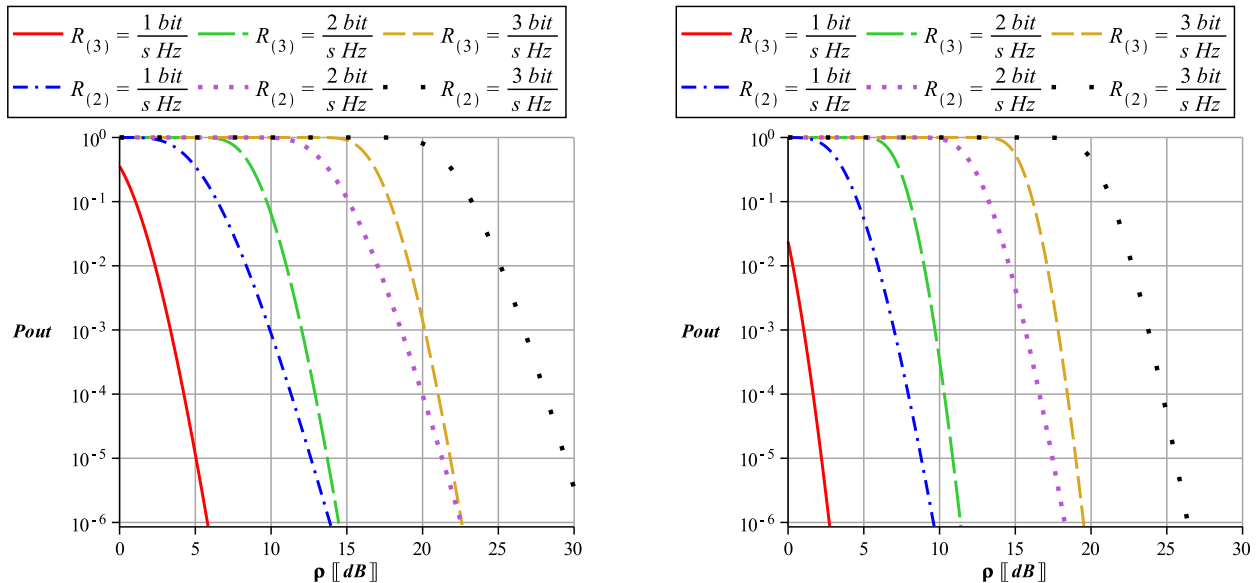


Figure 5: Outage probability for configurations (2) and (3) for  $N = 3$  and  $N = 4$  at different  $R$

and  $R = 2 \text{ bits/s/Hz}$  configuration (3) achieves outage probability of  $10^{-3}$  for  $\rho = 12 \text{ dB}$  and configuration (2) for  $\rho = 18.5 \text{ dB}$ . By increase of the number of antenna significantly better outage performance is achieved. For rate  $R = 2 \text{ bits/s/Hz}$  the outage probability of  $10^{-3}$  for the system with  $N = 3$  antenna is achieved at  $\rho = 12 \text{ dB}$  and for the system with  $N = 4$  antenna is achieved at  $\rho = 9.65 \text{ dB}$ . Moreover, the configuration (3) with  $N = 4$  antennas has significantly higher diversity gain ( $d = 16$ ) compared to the case where  $N = 3$  antennas ( $d = 9$ ).

## 5 Conclusions

In this paper, simple approximations of the ergodic capacity for DCF MIMO relaying with and without direct link are derived. By means of these approximations it is shown that the system with direct link has higher ergodic capacity.

For the non-ergodic channel, simple approximations of the outage probability for the considered configurations are derived. In the case of the system without direct link it is shown that results obtained by the approximation have good match with the results obtained by Monte Carlo simulations. Moreover, by means of these approximations it is shown that the system with direct link has significantly lower outage probability and higher diversity gain.

In all scenarios the increase of the number of antennas per node results in increase of the ergodic capacity, decrease of the outage probability and increase of the diversity gain.

## Appendix A

In the case of system configurations (1) and (2), the cumulative distribution function (CDF) of the instantaneous SNR is tightly approximated as [13, eq.(22)]:

$$\begin{aligned}
 F(\gamma) &= 1 + \frac{1}{\Gamma(m)} \sum_{k=0}^{m-1} \sum_{n=0}^{m-1} \frac{(-1)^{m+k+n} \Gamma(m-k) (2k+n-m+1)_{m-n-1}}{\Gamma(m-n)} \\
 &= \frac{(b+1)^n b^k}{\Gamma(k+1) \Gamma(n+1)} \left(\frac{\gamma}{\bar{\gamma}}\right)^{n+2k} \exp\left(-\frac{(b+1)\gamma}{\bar{\gamma}}\right)
 \end{aligned} \tag{32}$$

We approximate (32) by taking only the terms with  $k = 0$ , which yields

$$F(\gamma) \approx 1 - \sum_{n=0}^{m-1} \frac{(b+1)^n}{n!} \left(\frac{\gamma}{\bar{\gamma}}\right)^n \exp\left(-\frac{(b+1)\gamma}{\bar{\gamma}}\right). \tag{33}$$

The accuracy of such simplification is checked in [14] and [27] where it is shown that the results obtained with the simplified approximation are closely matched with the tight approximation (32) and the exact results obtained by numerical integration and Monte Carlo simulations.

We can express the second term of (33) through gamma and upper incomplete gamma function [35, eq.(8.350.2)] by usage of [35, eq.(8.352.2)]

$$\exp\left(-\frac{(b+1)\gamma}{\bar{\gamma}}\right) \sum_{n=0}^{m-1} \frac{(b+1)^n}{n!} \left(\frac{\gamma}{\bar{\gamma}}\right)^n = \frac{\Gamma\left(m, \frac{(b+1)\gamma}{\bar{\gamma}}\right)}{\Gamma(m)}. \tag{34}$$

If we introduce (34) in (33) we obtain the following expression for the CDF

$$F(\gamma) \approx 1 - \frac{\Gamma\left(m, \frac{(b+1)\gamma}{\bar{\gamma}}\right)}{\Gamma(m)}. \tag{35}$$

The function given in (35) is CDF of the random variable that is following the Gamma PDF with shape parameter  $m$  and scale parameter  $\theta = \bar{\gamma}/(b+1)$ , hence the instantaneous SNR of system configurations (1) and (2) is approximated by random variable which follows Gamma PDF given with (21).

## Appendix B

For derivation of (25) we assume that direct link is exposed to Rayleigh fading. In such case if the channel coefficients  $w_{ij}$  are circularly symmetric complex Gaussian random variables with zero mean and unit variance, the squared envelope of signal follows exponentially decaying PDF and the instantaneous SNR of the direct link  $\gamma_{31} = \bar{\gamma} \|\mathbf{W}\|_F^2$  follows Gamma PDF [13]. The instantaneous SNR of the indirect link  $\gamma_R = \gamma_{32} \gamma_{21} / (\gamma_{32} + \gamma_{21})$  is distributed by (21) in which

we select  $b = 1$  and  $m = N^2$  since we consider system configuration (3)

$$\begin{aligned} f_{31}(\gamma) &= \frac{1}{\bar{\gamma}^m \Gamma(m)} \gamma^{m-1} e^{-\frac{\gamma}{\bar{\gamma}}}, \\ f_R(\gamma) &= \frac{2^m}{\bar{\gamma}^m \Gamma(m)} \gamma^{m-1} e^{-\frac{2\gamma}{\bar{\gamma}}}. \end{aligned} \quad (36)$$

The resulting random variable is sum of two random variables each following Gamma PDF with different scale parameter:  $\gamma = \gamma_{31} + \gamma_R$  [34, eq.(16.18)]. In arbitrary case the sum of  $n$  random variables which follow Gamma PDFs is

$$Y = X_1 + X_2 + \dots + X_n, \quad f_i(x_i) = \frac{x_i^{m_i}}{\theta_i^{m_i} \Gamma(m_i)} e^{-\frac{x_i}{\theta_i}}. \quad (37)$$

The random variable  $Y$  is distributed by [37, eq.(2.4), eq.(2.5), eq.(2.8), eq.(2.9)]

$$\begin{aligned} g(y) &= C \sum_{k=0}^{\infty} \frac{\delta_k y^{\rho+k-1}}{\Gamma(\rho+k) \theta_l^{\rho+k}} e^{-\frac{y}{\theta_l}}, \quad \theta_l = \min_i(\theta_i), \quad \rho = \sum_{i=1}^n m_i, \\ C &= \prod_{i=1}^n \left(\frac{\theta_l}{\theta_i}\right)^{m_i}, \quad \delta_{k+1} = \frac{1}{k+1} \sum_{i=1}^{k+1} i \gamma_i \delta_{k+1-i}, \quad k = 0, 1, 2, \quad \delta_0 = 1, \\ \gamma_k &= \frac{1}{k} \sum_{i=1}^n m_i \left(1 - \frac{\theta_l}{\theta_i}\right)^k, \quad k = 1, 2, \dots \end{aligned} \quad (38)$$

We simplify the parameters given in (38) for the case of two random variables

$$\theta_l = \frac{\bar{\gamma}}{b+1}, \quad \rho = 2m, \quad C = (b+1)^{-m}, \quad \delta_i = \frac{(m)_i}{i!} \left(\frac{b}{b+1}\right)^i. \quad (39)$$

For the case of system configuration (3) where  $b = 1$  the parameters in (39) are

$$\theta_l = \frac{\bar{\gamma}}{2}, \quad \rho = 2m, \quad C = 2^{-m}, \quad \delta_i = \frac{(m)_i}{i!} \left(\frac{1}{2}\right)^i. \quad (40)$$

If parameters from (40) are introduced in the expression for  $g(y)$  in (38) we obtain (25).

## References

- [1] Sendonaris A, Erkip E, Aazhang B. User Cooperation Diversity Part I and Part II. IEEE Transactions on Communications 2003; 11: 1927-48.
- [2] Cover TM, Gamal AE. Capacity Theorem for the relay channels. IEEE Transactions on Information Theory 1979; 5.
- [3] Lee IH, Kim D. End-to-End BER Analysis for Dual-Hop OSTBC Transmissions over Rayleigh Fading Channels. IEEE Transactions on Communications 2008; 3.

- [4] Yi Z, Kim I-M. Approximate-BER-Distributed-Alamouti's Code in Dissimilar Cooperative Networks with Blind Relays. *IEEE Transactions on Comm.* 2009; 12.
- [5] Chen S, Wang W, Zhang X, Sun Z. Performance Analysis of OSTBC Transmission in Amplify-and-Forward Cooperative Relay Networks. *IEEE Transactions on Vehicular Technology* 2010; 1.
- [6] Lee IH, Kim D. Decouple-and-Forward Relaying for Dual-Hop Alamouti Transmissions. *IEEE Communications Letters* 2008; 2.
- [7] Lee IH, Kim D. Achieving Maximum Spatial Diversity with Decouple-and-Forward Relaying in Dual-Hop OSTBC Transmissions. *IEEE Tran. on W. Comm.* 2010; 3.
- [8] Duong TQ, Zepernick HJ, Tsiftsis TA. Amplify-and-Forward MIMO Relaying with OSTBC over Nakagami-m Fading Channels. *IEEE International Conference on Communications.* 2010.
- [9] Yang L, Zhang QT. Performance Analysis of MIMO Relay Wireless Networks With Orthogonal STBC. *IEEE Transactions on Vehicular Technology* 2010; 7.
- [10] Chen Y, Wu G, Lin W, Li Q, Li S. Outage Probability of Space-Time Coded Decouple-and-Forward Relaying over Nakagami-m Fading Channels. *International Conference on Wireless Communications. Networking and Mobile Computing.* 2009.
- [11] Abdaoui A, Ahmed MH. On the Performance Analysis of a MIMO-Relaying Scheme With Space-Time Block Codes. *IEEE Transactions On Vehicular Tech.* 2010; 7.
- [12] Dharmawansa P, McKay MR, Mallik RK. Analytical Performance of Amplify-and-Forward MIMO Relaying with Orthogonal Space-Time Block Codes. *IEEE Transactions on Communications* 2010; 7.
- [13] Stosic J, Hadzi-Velkov Z. Simple tight approximations of the error performance for dual-hop MIMO relay systems in Rayleigh fading. *AEÜ - International Journal of Electronics and Communications* 2013; 10: 854-960.
- [14] Stosic J, Hadzi-Velkov Z. Outage probability approximations for dual-hop Amplify-and-Forward MIMO relay systems in Rayleigh fading. *Proc. 11th International Conference on Telecommunication in Modern Satellite, Cable and Broadcasting Services (TELSIKS 2013)*, Nis, Serbia, 16-19. 2013.
- [15] Bhatnagar MR. On the Capacity of Decode-and-Forward Relaying over Rician Fading Channels. *IEEE Communications Letters* 2013; 6:1100-3.
- [16] Arti M.K., Bhatnagar MR. Maximal Ratio Transmission in AF MIMO Relay Systems Over Nakagami-m Fading Channels. *IEEE Transactions On Vehicular Tech.* 2015; 5.

- [17] Arti M.K., Bhatnagar MR. Performance Analysis of Hop-by-Hop Beamforming and Combining in DF MIMO Relay System over Nakagami-m Fading Channels. *IEEE Communications Letters* 2013; 11: 2080-83.
- [18] Arti M.K., Bhatnagar MR. Performance Analysis of Two-Way AF MIMO Relaying of OSTBCs With Imperfect Channel Gains. *IEEE Transactions On Vehicular Technology* 2014; 8: 4118-24.
- [19] Bhathagar MR, Arti M.K. Beamforming and Combining in Decode-and-Forward MIMO Relay Networks. *IEEE Communications Letters* 2013; 8: 1556-59.
- [20] Bansal A, Bhatnagar MR, Hjørungnes A, Han Z. Low-Complexity Decoding in DF MIMO Relaying System. *IEEE Trans. On Vehicular Technology* 2013; 3: 1123-37.
- [21] Arti M.K., Mallik RK, Schober R. Beamforming and Combining in Two-Way AF MIMO Relay Networks Fellow, *IEEE Communications Letters* 2013; 7: 1400-3.
- [22] Arti M.K., Mallik RK, Schober R. Joint Channel Estimation and Decoding of Space-Time Block Codes in AF MIMO Relay Networks. *International Conference on Signal Processing and Communications (SPCOM)*, Bangalore, India, 22-25 July. 2012.
- [23] Arti M.K., Mallik RK, Schober R. Channel Estimation and Decoding of OSTBC in Two-Way AF MIMO Relay Networks. *IEEE 78th Vehicular Technology Conference*, Las Vegas, NV, 2-5 Sept. 2013.
- [24] Arti M.K., Mallik RK, Schober R. Performance Analysis of OSTBC Relaying in AF MIMO Relay Systems With Imperfect CSI. *IEEE Transactions On Vehicular Technology* 2015; 7: 3291-98.
- [25] Stosic J, Hadzi-Velkov Z. Performance analysis of dual-hop MIMO systems. *Proc. 2nd Conference on Information and Communication Technologies' Innovations (ICT Innovations 2010)*, Ohrid, Macedonia, 12-15 September. 2010.
- [26] Stosic J, Hadzi-Velkov Z. Performance analysis of dual-hop dual-antennas MIMO systems in Rayleigh fading. *Proc. 2nd International Congress on Ultra Modern Telecommunications and Control Systems (ICUMT 2010)*, Moscow, 18-20 October. 2010.
- [27] Stosic J, Hadzi-Velkov Z. Approximate Performance Analysis of Dual-hop Decouple-and-Forward MIMO Relaying. *Proc. 11th International Conference on Electronics, Telecommunications, Automation and Informatics*, Ohrid, Macedonia, 26-28 September. 2013.
- [28] Simon MK, Alouini MS. *Digital Communication over Fading Channels*. Second Edition. New York: Wiley; 2005.
- [29] Hasna MO, Alouini MS. A Performance Study of Dual-Hop Transmissions With Fixed Gain Relays. *IEEE Transactions On Wireless Communications* 2004; 6.

- [30] Jafarkhani H. Space Time Coding Theory and Practice. Cambridge Un. Press; 2005.
- [31] Tarokh V, Jafarkhani H, Calderbank AR. Space-time block coding for wireless communications: Performance results. IEEE JSAC 1999; 3: 451-60.
- [32] Golub GH, Van Loan CF. Matrix Computations. Johns Hopkins Un. Press. 2012.
- [33] Tarokh V, Jafarkhani H, Calderbank AR. Space-time block codes from orthogonal designs. IEEE Transactions On Information Theory 1999; 5: 1456-67.
- [34] Gamal AE, Kim Y-H. Network Information Theory. Cambridge Un. Press; 2011.
- [35] Gradshteyn IS, Ryzhik IM. Table of Integrals, Series, and Products. 6th ed. Burlington USA: Academic Press; 2000.
- [36] Abramowitz M, Stegun IA. Handbook of Mathematical Functions with Formulas, Graphs, and Mathematical Tables. 9th edition. Dover; 1970.
- [37] Moschopoulos PG. The Distribution of the Sum of Independent Gamma Random Variables. Annals of the Institute of Statistical Mathematics 1985; 37.
- [38] Kramer G, Maric I, Yates RD. Cooperative Communications (Foundations and Trends in Networking). Now Publishers Inc; 2006.
- [39] Laneman J. N. , Tse D. N. C. Cooperative Diversity in Wireless Networks: Efficient Protocols and Outage Behavior. IEEE Trans. on Infor. Theory 2004; 12: 3062-80.
- [40] Papoulis A, Pillai SU. Probability Random Variables and Stochastic Processes. 4th Edition. McGraw-Hill Europe; 2002.
- [41] Knuth DE. Two notes on notation. American Mathematical Monthly 1992; 5.
- [42] Tse D, Viswanath P. Fundamentals of Wireless Communications. Cambridge University Press; 2005.
- [43] Goldsmith A. Wireless Communications. Cambridge University Press; 2005.
- [44] Sandhu S, Paulraj A. Space-Time Block Codes: A Capacity Perspective. IEEE Communications Letters 2000: 12.